academicJournals

Vol. 8(24), pp. 1298-1306, 30 June, 2013
DOI: 10.5897/IJPS2013.3922
ISSN 1992 - 1950 © 2013 Academic Journals
http://www.academicjournals.org/IJPS

International Journal of Physical Sciences

Full Length Research Paper

Linearization of Zoeppritz equations and practical utilization

Oladapo, Michael Ilesanmi

Department of Applied Geophysics, Federal University of Technology, Akure, Nigeria.

Accepted 21 June, 2013

The theory and practical utilization of simplification of the original general expressions for the reflection of compression and shear waves at a boundary as a function of the densities and velocities of layers in contact are presented in this paper. The original general expressions are highly non-linear and presumed to defy physical insight. Elimination of the properties of V_s and ΔV_s in favour of σ and $\Delta\sigma$ enabled the success of a two-term approximation and revealed the surprising effects of Poisson's ratio on P-wave reflection coefficient which was a neglected elastic constant. The simplified equation was further expressed in terms of angular reflections to obtain first order reflectivity expression in terms of R_p and R_s. The number of unknown parameters is thus reduced by assuming that the fractional changes in material parameters are small across layer interfaces. Simplification of the equation has brought into existence the Amplitude Variation Offset (AVO) attributes with successful practical utilization in hydrocarbon delineation in many oil fields including the Niger Delta Slope. Determination of the terms of the linearized equation from rock properties and seismic events remains of vital value in practice as demonstrated in the evaluation of hydrocarbon potential in North-Built field.

Key words: Compressional and shear waves, densities, velocities, Poisson's ratio, amplitude variation offset (AVO) attributes, hydrocarbon.

INTRODUCTION

Knott (1899) and Zoeppritz (1919) deduced the general expressions for the reflection of compression and shear waves at a boundary as a function of the densities and velocities of layers in contact. The unwieldy nature of the equations makes visualising how the variation of a particular parameter will affect the reflection coefficient curve very difficult (Castagna, 1993). Realising that the simplifications and approximations of the equations are desirable in order to apply them, Aki and Richards (1980) gave a more convenient form. This work is thus aimed at the practical utilization of the Zoeppritz equations approximations in North-Built field of the Niger Delta Slope.

The Zoeppritz's equations satisfying four boundary conditions are in the following forms (Sheriff and Geldart 1982):

$$A_1 \cos\theta_1 - B_1 \sin\phi_1 + A_2 \cos\theta_2 + B_2 \sin\phi_2 = A_0 \cos\theta_1 \quad (1)$$

$$A_1 \sin\theta_1 + B_1 \cos\phi_1 - A_2 \sin\theta_2 + B_2 \cos\phi_2 = A_0 \sin\theta_1 \quad (2)$$

$$A_1 Z_1 \cos 2\phi_1 - B_1 \omega_1 \sin 2\phi_1 - A_2 Z_2 \cos 2\phi_1 - B_2 \omega_2 \sin 2\phi_2 = -A_0 Z_1 \cos 2\phi_1 \quad (3)$$

$$A_1 \gamma_1 \omega_1 \sin 2\theta_1 + B_1 \omega_1 \cos 2\phi_1 + A_2 \gamma_2 \omega_2 \sin\theta_2 - B_2 \omega_2 \cos 2\phi_2 = A_0 \gamma_1 \omega_1 \sin 2\theta_1 \quad (4)$$

Where $Z_i = \rho_i V_{pi}; \quad \omega_i = \rho_i V_{si}$ (5)

E-mail: oladapom@yahoo.co.uk.

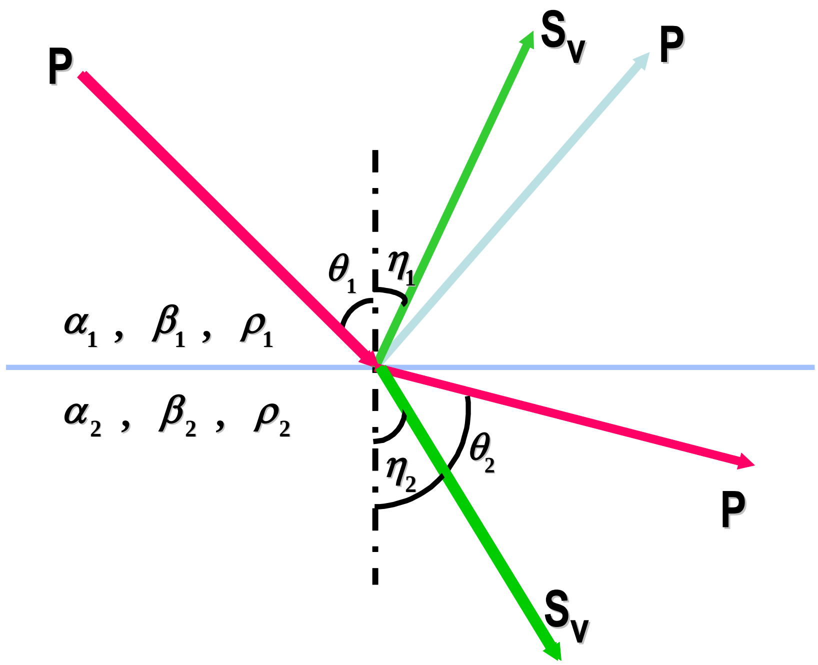

Figure 1. Stresses and displacement across the boundary of elastic media.

$$\gamma_i = \frac{\omega_i}{Z_i} = \frac{V_{si}}{V_{pi}} \quad i = 1, 2.....n \qquad (6)$$

These equations yield amplitudes that are accurate up to the critical angle as their description does not include head-wave energy (Sheriff, 2002). The equations assume continuity of stress and displacement at the interface.

At an interface, the densities and velocities in each of the media must be known, and then $Z_1, Z_2, \omega_1, \omega_2, \gamma_1$ and γ_2 can be derived. If A_0 and θ_1 are known, then θ_2, λ_2 *and* λ_1 can be computed to obtain amplitudes $A_1, A_2, B_1,$ *and* B_2.

For a normal incident P-wave, $\theta_1, \theta_2, \lambda_1$ *and* λ_2 reduce to zero hence $\cos\theta_1 = \cos\theta_2 = 1$, then $\sin\theta_1 = \sin\theta_2 = 0$.

In practice, detectors only respond to the longitudinal component of the waves, therefore, B_1 *and* B_2 do not exist. Thus:

$$A_1 + A_2 = A_0 \qquad (7)$$

That is $$T = \frac{2\rho_1 V_1}{\rho_1 V_1 + \rho_2 V_2} \qquad (8)$$

T is the transmission coefficient.

Therefore, $$R = \frac{A_1}{A_0} = \frac{\rho_2 V_2 - \rho_1 V_1}{\rho_2 V_2 + \rho_1 V_1} \qquad (9)$$

If the incident wave intercepts the interface obliquely, the situation becomes more complicated because the *R* is a tortuous function of the angle of incidence; the densities of the two bounding media; the ratio of velocities of the two media and the Poisson's ratio contrast of the two media (Figure 1).

Aki and Richards (1980) and Waters (1981) gave the equations in matrix form as:

$$\begin{bmatrix} \sin\theta & \cos\phi & -\sin\theta` & \cos\phi` \\ -\cos\theta & \sin\phi & -\cos\theta` & -\sin\phi` \\ \sin 2\theta & \frac{V_{p1}}{V_{s1}}\cos 2\phi & \frac{\rho_2 V_{s2}{}^2 V_{p1}}{\rho_1 V_{s1}{}^2 V_{p2}}\sin 2\theta` & -\frac{\rho_2 V_{s2} V_{p1}}{\rho_1 V_{s1}{}^2}\cos 2\phi` \\ \cos 2\theta & \frac{V_{s1}}{V_{p1}}\sin 2\phi & -\frac{\rho_2 V_{p2}}{\rho_1 V_{p1}{}^2}\cos 2\phi` & -\frac{\rho_2 V_{s2}}{\rho_1 V_{P1}{}^2}\sin 2\phi` \end{bmatrix} \begin{bmatrix} R_P \\ R_S \\ T_P \\ T \end{bmatrix} = \begin{bmatrix} -\sin\theta \\ -\cos\phi \\ \sin 2\theta \\ -\cos 2\phi \end{bmatrix} \qquad (10)$$

APPROXIMATION OF ZOEPPRITZ'S EQUATIONS

The Zoeppritz's equations are highly non-linear with respect to velocities and densities (Spratt et al., 1993). From the matrix description of the Zoeppritz equations, Aki and Richards (1980) derived the following formula:

$$R(\theta) \approx \frac{1}{2}\left(1 - 4\left(\frac{V_S}{V_P}\right)^2 \sin^2\theta\right)\frac{\Delta\rho}{\rho} + \frac{\sec^2\theta}{2}\frac{\Delta V_P}{V_P} - \left(\frac{4V_S}{V_P}\right)^2 \sin^2\theta\,\frac{\Delta V_S}{V_S}. \qquad (11)$$

Where the elastic properties are related as follows to those on each side of the interface

$$\Delta V_P = (V_{P2} - V_{P1}) \ \ and \ \ V_P = (V_{P2} + V_{P1})/2 \tag{12}$$

$$\Delta V_S = \left(V_{S2} - V_{S1}\right) \ \ and \ \ V_S = \left(V_{S2} + V_{S1}\right)/2 \tag{13}$$

$$\Delta\rho = \left(\rho_2 - \rho_1\right) \ \ and \ \ \rho = \left(\rho_2 + \rho_1\right)/2 \tag{14}$$

The angle □ is the average of incidence and transmission angles $\theta = \left(\theta_2 + \theta_1\right)/2$.

By proposing a polynomial fit for the reflectivity that is accurate for an angle of incidence up to 35°, Shuey (1985) modified Equation (11) by eliminating the properties $V_S, \ \Delta V_S$ in favour of σ, Δσ

$$\Delta\sigma = \left(\sigma_2 - \sigma_1\right) \ \ and \ \ \sigma = \left(\sigma_2 + \sigma_1\right)/2 \tag{15}$$

The substitution is effected using the equation

$$V_S{}^2 = V_P{}^2 \frac{1 - 2\sigma}{2(1-\sigma)} \tag{16}$$

R_0 and the amplitude at NI were factored out by the differential of Equation (11) thus resulting in

$$R(\theta)/R_0 \approx 1 + A\sin^2\theta + B\left(\tan^2\theta - \sin^2\theta\right) \tag{17}$$

Where,

$$R_0 = \frac{1}{2}\left(\frac{\Delta V_P}{V_P} + \frac{\Delta\rho}{\rho}\right) \tag{18}$$

$$A = A_0 + \frac{1}{(1-\sigma)^2}\frac{\Delta\sigma}{R_0} \tag{19}$$

$$A_0 = B - 2(1+B)\frac{1-2\sigma}{1-\sigma} \tag{20}$$

and

$$B = \frac{\Delta V_P / V_P}{\Delta V_P / V_P + \Delta\rho/\rho} \tag{21}$$

Multiplying Equation (17) through by R_0

$$R(\theta) \approx R_0 + \left[A_0 R_0 + \frac{\Delta\sigma}{(1-\sigma)^2}\right]\sin^2\theta + \frac{1}{2}\frac{\Delta V_P}{V_P}\left(\tan^2\theta - \sin^2\theta\right) \tag{22}$$

Equation (22) displays, which combinations of elastic properties are effective in successive ranges of angle θ. The first term gives the amplitude at normal incidence $(\theta = 0)$, the second term characterises *R (θ)* at intermediate angles, and the third term describes the approach to critical angle.

Castagna et al. (1998) adopted Swan, (1993) approach to express the Aki and Richards (1980) (Equation 12) for the Richards and Frasier (1976) approximation in terms of the angular reflections A, B and C:

$$R(\theta) \approx A + B\sin^2(\theta) + C\sin^2(\theta)\tan^2(\theta) \tag{23}$$

where

$$A = \frac{1}{2}\left(\frac{\Delta V_P}{V_P} + \frac{\Delta\rho}{\rho}\right); \tag{24}$$

$$B = \frac{1}{2}\frac{\Delta V_P}{V_P} - 2\left(\frac{V_S}{V_P}\right)^2\left(2\frac{\Delta V_S}{V_S} + \frac{\Delta\rho}{\rho}\right); \tag{25}$$

$$C = \frac{1}{2}\frac{\Delta V_P}{V_P} \tag{26}$$

Spratt et al. (1993) derived the first order reflectivity expressions from Equation (11) (in order to reduce the number of parameters that can be uniquely found) by assuming that the fractional changes in material parameters are small across the interface.

Assuming the incident angle is small while only terms to first order in $\sin^2\theta$ are retained, Equation (13) becomes:

$$R(\theta) = \frac{1}{2}\left[1 - 4\left(\frac{V_S}{V_P}\right)^2\sin^2\theta\right]\frac{\Delta\rho}{\rho} + \frac{1}{2}\left(1 + \sin^2\theta\right)\frac{\Delta V_P}{V_P} - 4\left(\frac{V_S}{V_P}\right)^2\frac{\Delta V_S}{V_S}\sin^2\theta \tag{27}$$

Rearranging the terms gives:

$$R(\theta) = \frac{1}{2}\left(\frac{\Delta\rho}{\rho} + \frac{\Delta V_P}{V_P}\right) + \left[\frac{1}{2}\left(\frac{\Delta\rho}{\rho} + \frac{\Delta V_P}{V_P}\right) - 8\left(\frac{V_S}{V_P}\right)^2\frac{1}{2}\left(\frac{\Delta\rho}{\rho} + \frac{\Delta V_P}{V_P}\right)\right]\sin^2\theta + \left[2\left(\frac{V_S}{V_P}\right)^2 - \frac{1}{2}\right]\frac{\Delta\rho}{\rho}\sin^2\theta$$

or

$$R(\theta) = R_P + (R_P - 2 * R_S)\sin^2\theta + 0 * \frac{\Delta\rho}{\rho}\sin^2\theta \tag{28}$$

where

$$R_P = \frac{1}{2}\left(\frac{\Delta\rho}{\rho} + \frac{\Delta V_P}{V_P}\right), \ R_S = \frac{1}{2}\left(\frac{\Delta\rho}{\rho} + \frac{\Delta V_S}{V_S}\right), \ \ 2* = 8\left(\frac{V_S}{V_P}\right)^2, \ \ 0* = 2\left(\frac{V_S}{V_P}\right)^2 - \frac{1}{2}.$$

R_P *and* R_S are the compression and shear reflectivity respectively (correct to first order in the Δ's).

If $\frac{V_P}{V_S}$ = 2, then 2* = 2 and 0* = 0 and the expression reduces to

$$R(\theta) \approx R_P + (R_P - 2R_S)\sin^2\theta \quad (29)$$

In most sedimentary basins, small changes in density can be expressed as small changes in (compressional) velocity, (Ross, 2000) such that

$$\frac{\Delta\rho}{\rho} \approx \frac{g\Delta V_P}{V_P} \quad (30)$$

Where $g = 0.25\left[2\left(\frac{V_s}{V_p}\right) - \frac{1}{2}\right]$ is an expansion coefficient for other effects in higher-order corrections. Using Equation (30), (24) and (25) can be rewritten as Equations (31) and (32) respectively assuming $\frac{V_p}{V_s}$ remains constant;

$$A = \frac{5}{8}\frac{\Delta V_P}{V_P} \quad (31)$$

$$B = \frac{4}{5}A - 2\gamma^2\left(2\frac{\Delta V_S}{V_S} + \frac{2}{5}A\right) \quad (32)$$

By substituting equation (31) into equation (32) and letting $\frac{V_S}{V_P}$ = γ,

$$B = \frac{1}{2}\frac{\Delta V_P}{V_P} - 2\left[\frac{V_S}{V_P}\right]^2\left(2\frac{\Delta V_S}{V_S} + \frac{1}{4}\frac{\Delta V_P}{V_P}\right) \quad (33)$$

which can be further reduced to

$$B = \frac{4}{5}A(1-\gamma)^2 - 4\gamma^2\frac{\Delta V_s}{V_s} \quad (34)$$

The simplification of the P-wave reflection coefficient given by Zoeppritz to various expressions (Equations 12 to 34) has enabled the determination and application of what is popularly referred to as Amplitude Variation with Offset (AVO) attributes. The three most commonly used approximations are:

$$R(\theta) \approx A + B\sin^2(\theta) \quad (35)$$

$$R(\theta) \approx R_p\left(1 + \tan^2\theta\right) - 2R_s\sin^2\theta \quad (36)$$

$$R(\theta) \approx NI\cos^2\theta + PR\sin^2\theta \quad (37)$$

Where, R = reflection coefficient; θ = angle of incidence; A = AVO intercept; B = AVO gradient.

Equation (35) is the original two-term Shuey (1985) equation, where the higher terms have been dropped by limiting the angle of incidence to θ < 30°. Equation (36) was introduced by Fatti et al. (1994) while Verm and Hilterman (1995) introduced Equation (37). A is the normal incidence (NI) attribute while B is the Poisson Reflectivity (PR) attribute.

Within the range of incidence angles (up to 35°) typically used in exploration (Seriff et al., 1980), Equations (35) to (37) can be considered equivalent, hence we have:

$$A = NI = R_p \quad (38a)$$

$$B = R_p - 2R_s \quad (38b)$$

$$R_s = \frac{A-B}{2} \quad \text{Pseudoshear} \quad (38c)$$

$$PR = 2\left(R_p - R_s\right) = A + B \quad (38d)$$

R_s is normal incidence S-wave reflection coefficient which is called pseudo shear because it is strictly the shear only when V_p/V_s = 2 (Hendrickson et al. 1991). From the approximations of Zoeppritz's equations, determination of A and B values of the linearized version of the equation becomes imperative. This can be obtained from rock property measurements in well logs (Oladapo and Adetola, 2005) and seismic events (Figure 2).

PRACTICAL UTILIZATION

Ostrander (1984) in the first practical approach to AVO, proposed a method that could distinguish between gas-related amplitude anomalies and non-gas-related anomalies. The change in zero-offset reflectivity R_0, or intercept, is the most diagnostic feature. The seismic response depends on the encasing geology, porefill, and interference effects (Veeken and Rauch-Davies, 2006). AVO interpretation may be enhanced by cross plotting

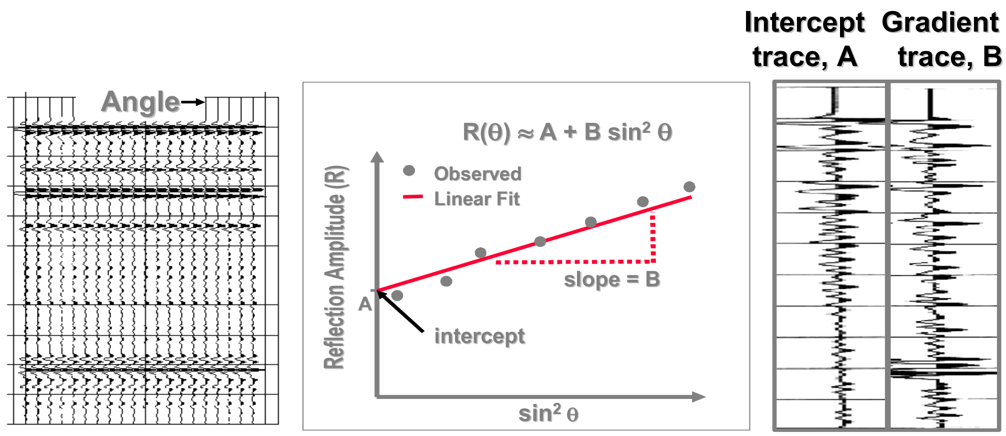

Figure 2. AVO Gradient and intercept.

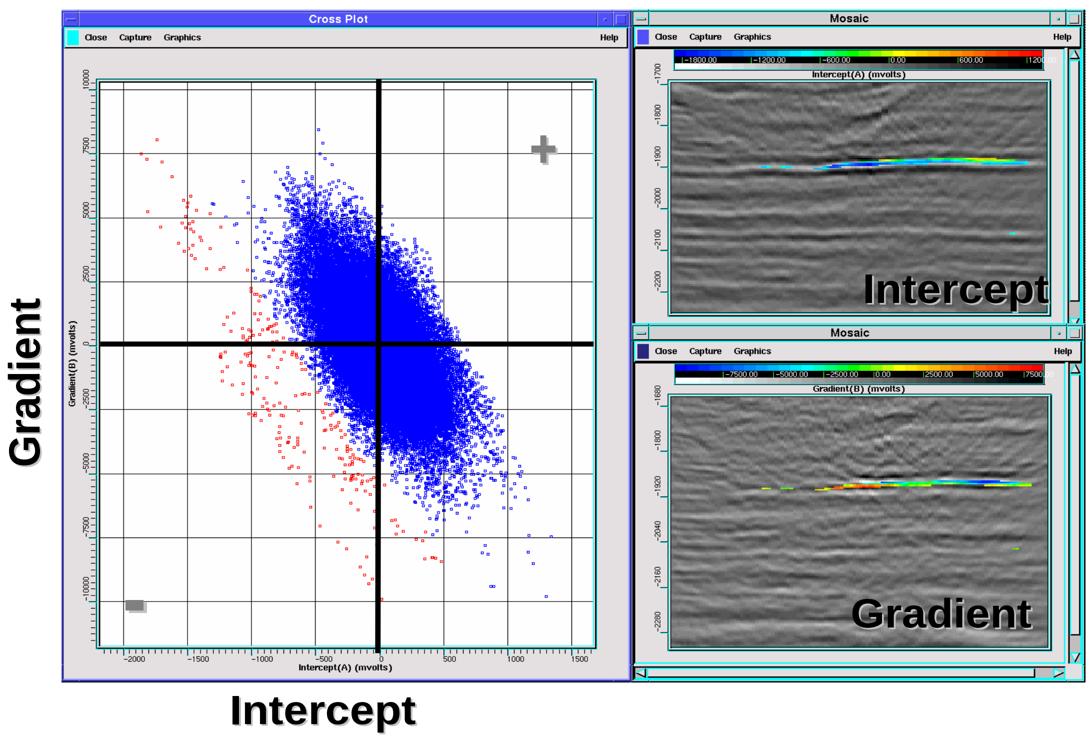

Figure 3. AVO Crossplot from a Niger Delta slope prospect. The highlighted points (red) on the crossplot indicate points that are anomalous due to fluid effects.

the AVO NI (Normal Incidence) intercept (A) and gradient RP (Poisson Reflectivity) (B) two parameters obtained from Shuey's two-term approximation of Zoeppritz's equations (Smith and Gidlow, 1987; Foster et al., 1993; Ross, 2000; Veeken et al., 2002; Oladapo et al., 2009; Kim et al., 2011; Hossain et al., 2012). Under a variety of reasonable petrophysical assumptions, brine-saturated sandstones and shale follow a well-defined "background" trend in an Intercept-Gradient plane. Hilterman (1987) observed that A and B are generally negatively correlated for background rocks. Deviations from the background trend may be indicative of hydrocarbons or lithology with anomalous properties. Typical attributes crossplot from Niger Delta Slope field is presented in Figure 3.

In the Niger Delta, AVO analyses have been successfully utilized for the detection and mapping of gas (Osuntola et al., 1997; Oladapo et al., 2009). A semi quantitative AVO analysis of a horizon (termed BB within

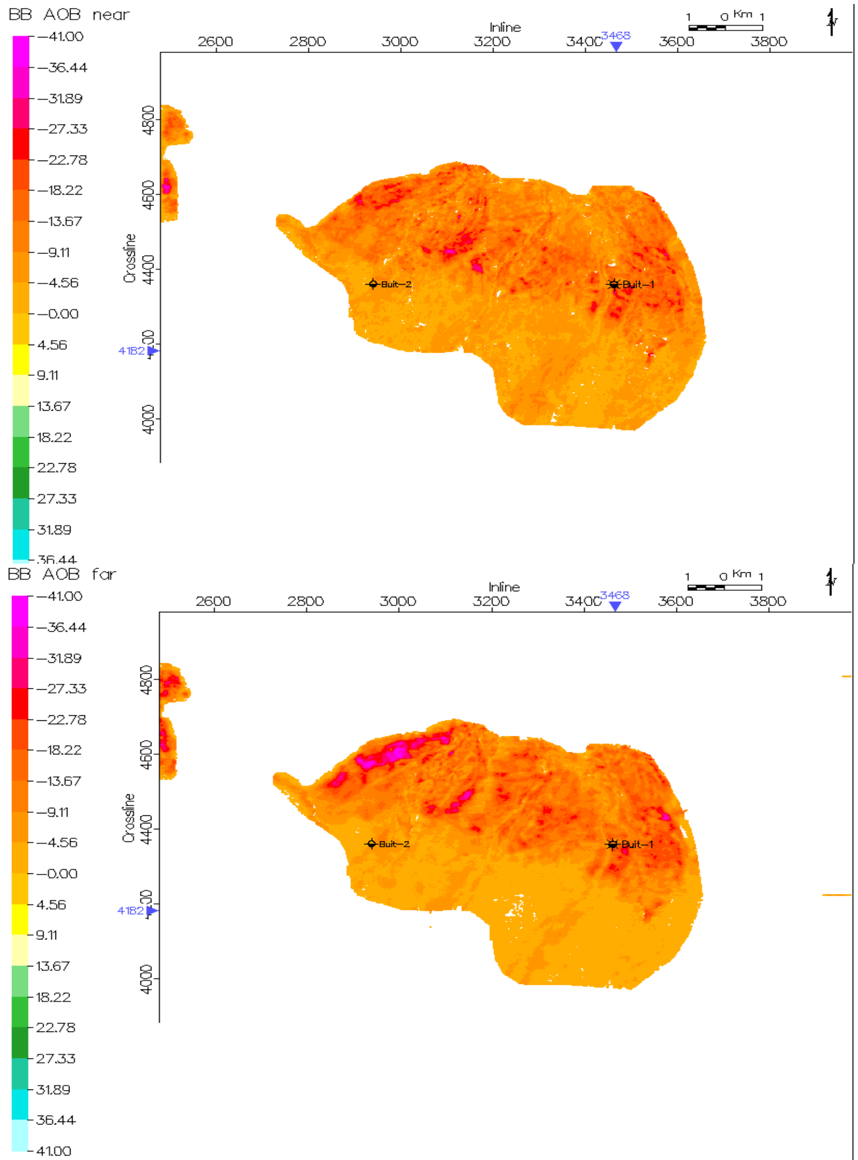

Figure 4. Sub-Stacks Amplitude maps of Buit-BB horizon.

time window of 2.668 s) within Buit North field of Niger Delta Slope was evaluated using the two parameter AVO attributes. Applications of Intercept and Gradient for Buit-North Field Evaluation are:

Near amplitude $$a_n = A + B\sin^2\theta_n \quad (39)$$

Far amplitude $$a_f = A + B\sin^2\theta_f \quad (40)$$

Solving this for B and for A for near and far stack:

$$a_f - a_n = B\left(\sin^2\theta_f - \sin^2\theta_n\right)$$

$$B = \frac{\left(a_f - a_n\right)}{\left(\sin^2\theta_f - \sin^2\theta_n\right)} \quad (41)$$

$$A = \frac{a_f \sin^2\theta_n - a_n \sin^2\theta_f}{\sin^2\theta_n - \sin^2\theta_f} \quad (42)$$

Pairs of far and full, and the near and far offset data (using Equations 39 and 40) were utilised for generating BB horizon substacks maps (Figure 4). The average angles used for the sub-stacks are near 10°, far 22.5°, full 27.5°. Using Amplitude/Background normal (a/b or AOB) approach, Equations 39 and 40 becomes:

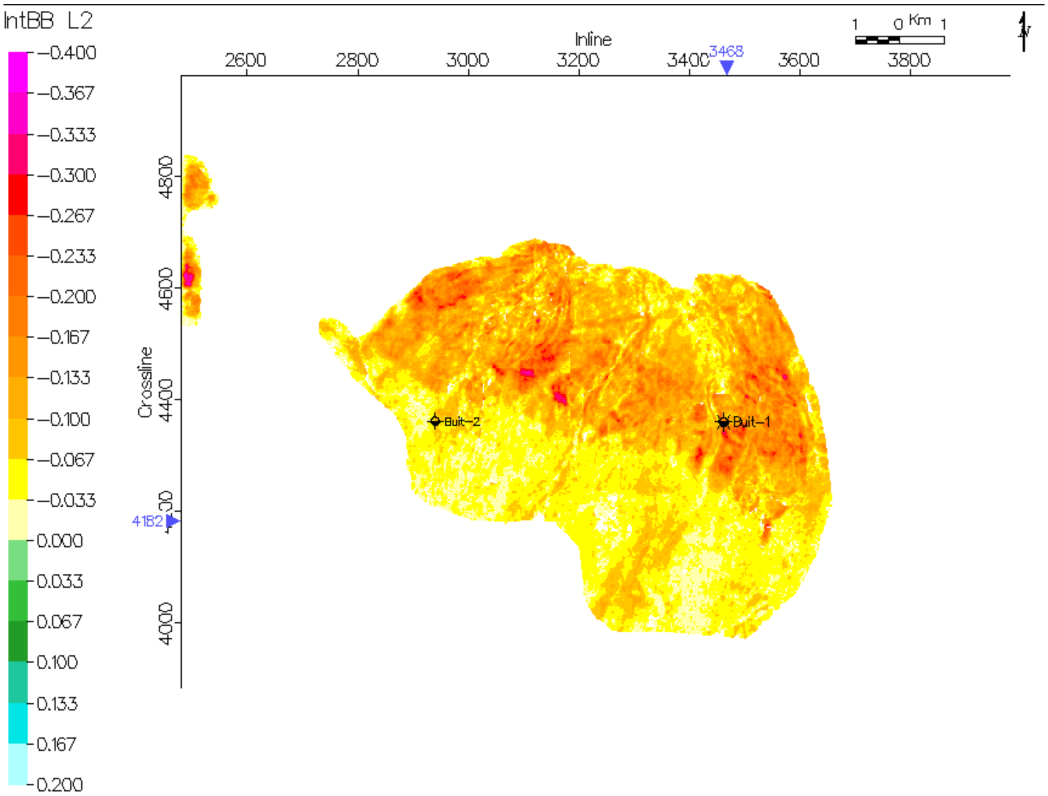

Figure 5. Intercept (A) amplitude map of Buit-BB horizon.

$$a/b_{near} = A + B\sin^2\theta_{near} \quad (43)$$

$$a/b_{far} = A + B\sin^2\theta_{far} \quad (44)$$

$$B = \frac{(a/b_{far} - a/b_{near})}{(\sin^2\theta_{far} - \sin^2\theta_{near})} \quad (45)$$

$$A = \frac{a/b_{far}\sin^2\theta_{near} - a/b_{near}\sin^2\theta_{far}}{\sin^2\theta_{near} - \sin^2\theta_{far}} \quad (46).$$

Similar computations were undertaken for the full and far data. The average of the two results utilised for generating Intercept and Gradient maps (designated L and M respectively) shown in Figures 5 and 6 are as follows:

$$B = \frac{a/b_{near}}{2(\sin^2\theta_{near} - \sin^2\theta_{far})} + \frac{a/b_{full}}{2(\sin^2\theta_{full} - \sin^2\theta_{far})} - a/b_{far}\frac{[(\sin^2\theta_{full} - \sin^2\theta_{far}) + (\sin^2\theta_{near} - \sin^2\theta_{far})]}{[(\sin^2\theta_{full} - \sin^2\theta_{far})(\sin^2\theta_{near} - \sin^2\theta_{far})]} \quad (47)$$

$$A = a/b_{far}\left[1 + \left(\frac{\sin^2\theta_{far}}{2(\sin^2\theta_{near} - \sin^2\theta_{far})}\right) + \left(\frac{\sin^2\theta_{far}}{2(\sin^2\theta_{full} - \sin^2\theta_{far})}\right)\right] - a/b_{near}\left(\frac{\sin^2\theta_{far}}{2(\sin^2\theta_{near} - \sin^2\theta_{far})}\right) - A/B_{full}\left(\frac{\sin^2\theta_{far}}{2(\sin^2\theta_{full} - \sin^2\theta_{far})}\right) \quad (48)$$

The above equations exhibit the dependence of intercept and gradient on a/b (AOB) values of near, far and full stack. The computation is analogous to regression with four points, once for near and full and twice for far stack. The horizon is characterised by higher amplitudes on both the intercept and gradient sections that are diagnostic of class III gas sand using the classifications of Rutherford and Williams (1989). The seismic attribute A (or L), B (or M) and Background normal (Bn) maps (Figures 4, 5, 6 and 7) show rising AVO profiles within the horizon.

Conclusion

These semi-quantitative AVO tools are effective hydrocarbon indicators (HCI) as displayed within BB horizon. Hydrocarbon potential rating (which is apparently higher at the north-western flank of the field) can be achieved using the approximation attributes. This

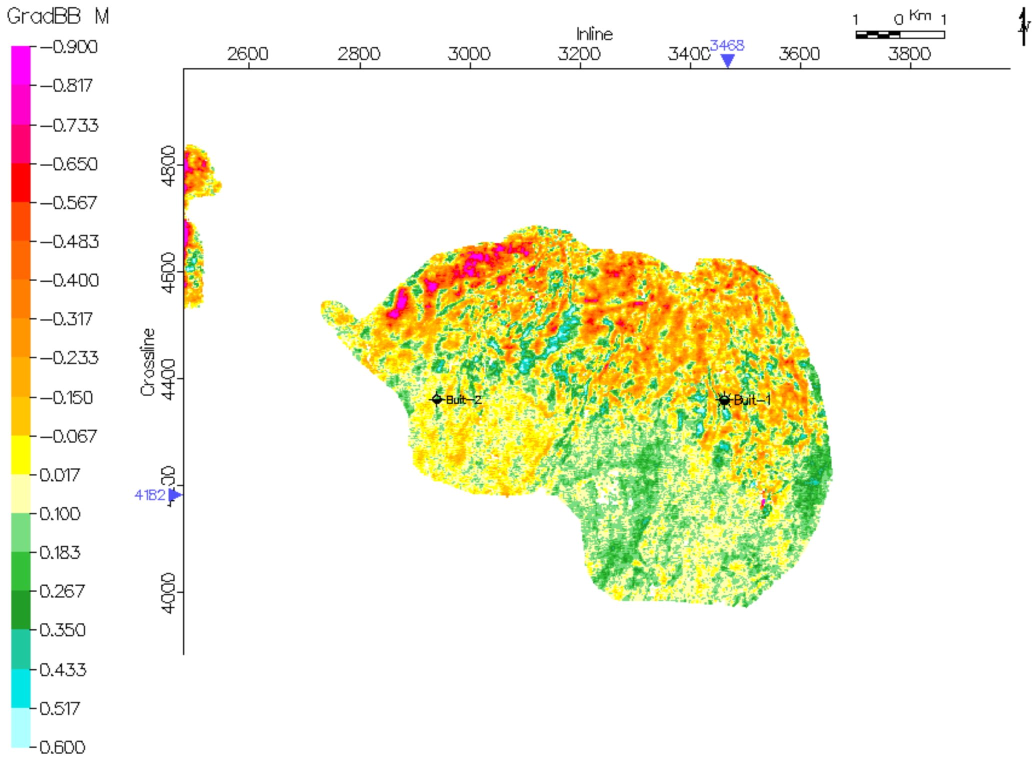

Figure 6. Gradient (B) map of Buit-BB horizon.

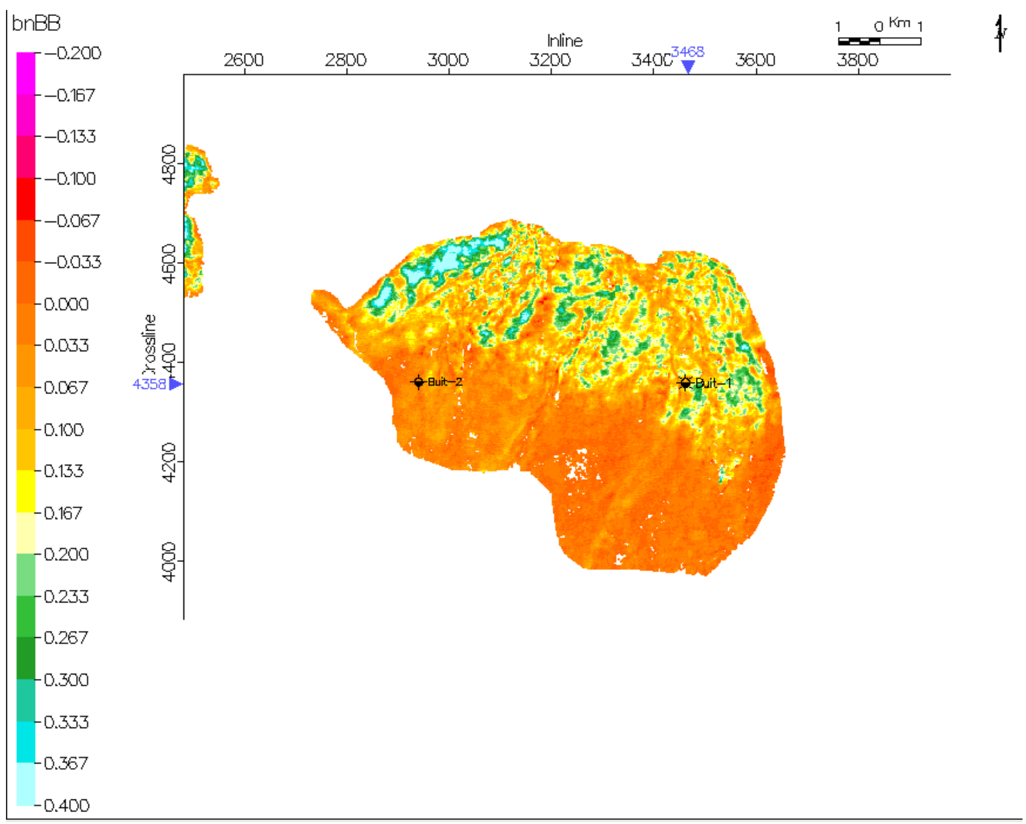

Figure 7. Background normal (bn) map of Buit-BB horizon.

assumption is based on the consistently higher AVO profile (AVO gradient and normal incidence amplitude) characterising the north-western section of the horizon.

REFERENCES

Aki K, Richards PG (1980). Quantitative Seismology: Theory and Methods. W.H. Freeman and Co.

Castagna JP (1993). Petrophysical imaging using AVO. The Leading Edge, 12(3):172-178.

Castagna JP, Swan HW, Foster JD (1998). Framework for AVO gradient and intercept interpretation: Geophysics 63:948–956.

Fatti JL, Smith GC, Vail PJ, Levitt PR (1994). Detection of gas in sandstone reservoirs using AVO analysis: A 3-D seismic case history using the Geostack technique. Geophysics 59:362-1376.

Hendrickson JS, Li SM, Daste AS, Gunther GL (1991). Evidence for AVO as a direct hydrocarbon indicator and a direct no-hydrocarbon indicator. Shell Geophysical conference paper No. 100.

Hossain Z, Mukerji T, Fabricius IL (2012). Vp-Vs relationship and amplitude variation with offset modelling of glauconitic greensand‡. Geophysical Prospecting, 60:117–137. doi: 10.1111/j.1365-2478.2011.00968.x

Kim JS, Won-Ki K, Hee-Sang H, Sung-Soo K (2011). AVO analysis using crossplot and amplitude polynomial methods for characterisation of hydrocarbon reservoirs Exploration Geophysics 42(1):25-41 http://dx.doi.org/10.1071/EG10048

Knott CG (1899). Reflection and refraction of elastic waves, with seismological applications. Phil. Mag., 5th ser. 48:64–97.

Oladapo MI, Adetola BA (2005). Rock property trend analyses in the Niger Delta Slope. Nanjing Institute of Geophysical Prospecting and Institute of Physics Publishing. J. Geophys. Eng. 2:103–110.

Oladapo MI, Ojo JS Olorunfemi MO, Adetola BA (2009). Monte-Carlo Modeling of Some Niger Delta Slope Events. J. Appl. Sci. 9(5):883-891.

Ostrander WJ (1984). Plane-wave reflection coefficients for gas-sands at non-normal angles of incidence: Geophysics 49:1637- 1648.

Osuntola OK, Ojo JS, Maxwell BA (1997). Interpreting the Amplitude Versus Offset (AVO) analysis results. Paper presented at the 15th Annual Conference of the Nigerian Association of Petroleum Explorationists.

Richards PG, Frasier CW (1976). Scattering of elastic wave from depth-dependent inhomogeneities: Geophysics, 41:441 – 458.

Ross CP (2000). Effective AVO crossplot modelling: A tutorial. Geophysics 65:700-711.

Rutherford SR, Williams RH (1989). Amplitude-versus Offset variations in gas sands: Geophysics, 54:680–688.

Seriff AJ, Thayer RE, Sriram KP, Cooper MR (1980). Vp and Vs of sedimentary rocks, Items 230-13102.00, Monthly Research Summary, Shell Development Bellaire Research Center, Houston, November.

Sheriff RE, Geldart LP (1982). Exploration Seismology. Volume 1, Cambridge University Press.

Sheriff RE (2002). Encyclopedic Dictionary of Exploration Geophysics, 4th edn. SEG, Tulsa.

Shuey RT (1985). A simplification of the Zoeppritz equations: Geophysics, 50:609–614.

Smith JC, Gidlow PM (1987). Weighted stacking for rock property estimation and detection of gas. Geophys. Prospecting 35:993–1014.

Spratt RS, Goins NR, Fitch TJ (1993). Pseudo-Shear—The Analysis of AVO in Castagna, J.P., and Backus, M.M., Eds., Offset-dependent Reflectivity-Theory and Practice of AVO analysis: Soc. Expl. Geophys., 37-56.

Swan HW (1993). Properties of direct AVO hydrocarbon indicators in Castagna, J.P., and Backus, M.M., Eds., Offset-dependent Reflectivity-Theory and Practice of AVO analysis: Soc. Expl. Geophys. 78–92.

Veeken PCH, Rauch M, Gallardo R, Guzman E, Vila Villasenor R (2002). Seismic inversion of the Fortuna National 3D survey, Tabasco, Mexico. First Break 20:287–294.

Veeken Paul, Marianne Rauch-Davies (2006). AVO attribute analysis and seismic reservoir characterization. First Break 24:41-52.

Verm R, Hilterman F (1995). Lithology color-coded seismic sections: The calibration of AVO crossplotting to rock properties. The Leading Edge, 14(8):847-853.

Waters KH (1981). Reflection Seismology: A tool for energy resource exploration: John Wiley & Sons, Inc.

Zoeppritz K (1919). Erdbebenwellen VIII B, Über Reflexion ad Durchgang seismischer wellen durch Unstetigkeitsflachen: Göttinger Nach. 66-84.